Carcinogenesis, 2019, Vol. 40, No. 12, 1545–1556

doi:10.1093/carcin/bgz155
Advance Access Publication September 26, 2019
Original Article

ORIGINAL ARTICLE

Reversal of the Warburg phenomenon in chemoprevention of prostate cancer by sulforaphane

Krishna B. Singh[1], Eun-Ryeong Hahm[1], Joshi J. Alumkal[2,3], Lesley M. Foley[4], T.Kevin Hitchens[4,5], Sruti S. Shiva[1,6], Rahul A. Parikh[7], Bruce L. Jacobs[8] and Shivendra V. Singh[1,9,*]

[1]Department of Pharmacology and Chemical Biology, University of Pittsburgh School of Medicine, Pittsburgh, PA, USA, [2]Knight Cancer Institute, Oregon Health and Science University, Portland, OR, USA, [3]Rogel Cancer Center, University of Michigan, Ann Arbor, MI, USA, [4]Animal Imaging Center, [5]Department of Neurobiology and [6]Vascular Medicine Institute, University of Pittsburgh School of Medicine, Pittsburgh, PA, USA, [7]Department of Oncology, Kansas University Medical Center, Kansas City, KS, USA and [8]Department of Urology and [9]UPMC Hillman Cancer Center, University of Pittsburgh School of Medicine, Pittsburgh, PA, USA

*To whom correspondence should be addressed. Tel: +1 412 623 3263; Fax: +1 412 623 7828; Email: singhs@upmc.edu

Abstract

Inhibition of metabolic re-programming represents an attractive approach for prevention of prostate cancer. Studies have implicated increased synthesis of fatty acids or glycolysis in pathogenesis of human prostate cancers. We have shown previously that prostate cancer prevention by sulforaphane (SFN) in Transgenic Adenocarcinoma of Mouse Prostate (TRAMP) model is associated with inhibition of fatty acid metabolism. This study utilized human prostate cancer cell lines (LNCaP, 22Rv1 and PC-3), two different transgenic mouse models (TRAMP and Hi-Myc) and plasma specimens from a clinical study to explore the glycolysis inhibition potential of SFN. We found that SFN treatment: (i) decreased real-time extracellular acidification rate in LNCaP, but not in PC-3 cell line; (ii) significantly downregulated expression of hexokinase II (HKII), pyruvate kinase M2 and/or lactate dehydrogenase A (LDHA) *in vitro* in cells and *in vivo* in neoplastic lesions in the prostate of TRAMP and Hi-Myc mice; and (iii) significantly suppressed glycolysis in prostate of Hi-Myc mice as measured by *ex vivo* ^{1}H magnetic resonance spectroscopy. SFN treatment did not decrease glucose uptake or expression of glucose transporters in cells. Overexpression of c-Myc, but not constitutively active Akt, conferred protection against SFN-mediated downregulation of HKII and LDHA protein expression and suppression of lactate levels. Examination of plasma lactate levels in prostate cancer patients following administration of an SFN-rich broccoli sprout extract failed to show declines in its levels. Additional clinical trials are needed to determine whether SFN treatment can decrease lactate production in human prostate tumors.

Introduction

Metabolic deregulation is now regarded as one of the hallmarks of different malignancies including prostate cancer, which is a leading cause of cancer-related death in men in the United States and other Western countries (1,2). Earlier studies implicated increased *de novo* synthesis of fatty acids, which is very low in most normal tissues including the prostate gland, in pathogenesis of human prostate cancer (3,4). This hypothesis was corroborated by studies showing overexpression of fatty acid synthase (FASN) complex that catalyzes the terminal steps of the *de novo* fatty acid synthesis, in early [prostatic intraepithelial neoplasia (PIN)] as well as in late-stage prostate cancers (5). The expression of FASN was shown to be higher by ~5.7-fold in human PIN lesions when compared with the normal prostate tissue (5). These results indicated that overexpression

Received: 26 February 2019; **Revised:** 23 August 2019; **Accepted:** 18 September 2019

Abbreviations

ANOVA	analysis of variance
AR	androgen receptor
caAkt	constitutively active Akt
Cr	creatine
DMSO	dimethyl sulfoxide
ECAR	extracellular acidification rate
FASN	fatty acid synthase
GLUT	glucose transporter
HKII	hexokinase II
Lac	lactate
LDHA	lactate dehydrogenase A
MCT1	monocarboxylate transporter 1
MI	myo-inositol
PIN	prostatic intraepithelial neoplasia
PKM2	pyruvate kinase M2
PSA	prostate-specific antigen
SFN	sulforaphane
SFN-BSE	sulforaphane-rich broccoli sprout extract
TRAMP	Transgenic Adenocarcinoma of Mouse Prostate

of FASN, and hence increased *de novo* synthesis of fatty acids, was an early event in prostate carcinogenesis (5). Moreover, overexpression of FASN in prostate of transgenic mice resulted in development of PIN lesions (6). Inhibition of FASN as well as other enzymes of the fatty acid synthesis pathway pharmacologically or through genetic knockdown (RNA interference) inhibited growth of prostate cancer cells by induction of apoptosis (7–9). Clinical development of fatty acid synthesis inhibitors continues to be a priority for treatment of cancers (10).

Accumulating evidence indicates that human prostate cancer is a metabolically heterogeneous disease characterized by increased glycolysis in a subset of patients (11–15). Increased tumor glycolysis even under normoxic conditions is a phenomenon common to many cancers and first observed by Dr Otto Warburg several decades ago (16–18). Using ^{1}H high-resolution magic angle spinning spectroscopy of snap-frozen prostate biopsies, Tessem *et al.* (11) observed a highly significant increase in lactate levels in prostate cancer biopsies compared with benign tissue. Integrated metabolic profiling of oncogenically transformed human prostate epithelial cells and prostate tumor specimens from transgenic mice and humans also revealed enrichment of glycolysis intermediates in a subset of patients (13). Overexpression of lactate dehydrogenase A (LDHA), which catalyzes the final step of aerobic glycolysis, has been reported in clinical prostate cancer specimens in comparison with benign prostate hyperplasia (15). Therefore, an agent with the ability to simultaneously inhibit both fatty acid synthesis and glycolysis is attractive to prevent metabolically heterogeneous prostate cancer.

Natural products continue to be investigated for targeting cell metabolism for possible prevention and treatment of prostate cancer (19). Sulforaphane (SFN) and SFN-rich broccoli sprout extract (SFN-BSE), which have been investigated clinically for modulation of androgen receptor (AR) activity in prostate cancer patients with biochemical recurrence (20,21), are known to inhibit growth of prostate cancer cells preclinically in both therapeutic and preventative settings *in vivo* without any overt side effects (22–25). In one study, SFN administration significantly inhibited the *in vivo* growth of PC-3 cells implanted in male athymic mice (22). Prostate cancer prevention by dietary administration of SFN-BSE has also been documented in the Transgenic Adenocarcinoma of Mouse Prostate (TRAMP) mouse model (24).

We have shown previously that SFN treatment inhibits fatty acid synthesis in human prostate cancer cells *in vitro* and in prostate adenocarcinoma of TRAMP mice *in vivo* (26). We also found a significant decrease in plasma and prostate adenocarcinoma levels of acetyl-CoA, which is the building block of fatty acid synthesis and partly derived from glycolysis intermediates (3), in SFN-treated TRAMP mice in comparison with control (26). Therefore, it was of interest to determine whether SFN inhibits glycolysis. Another rationale for this study was that SFN treatment inhibits transcriptional activity of Myc, an oncogene known to regulate tumor glycolysis (27,28). The present study utilized human prostate cancer cell lines (LNCaP, 22Rv1 and PC-3 cells), two different transgenic mouse models (TRAMP and Hi-Myc) and plasma specimens from a clinical study to explore the glycolysis inhibition potential of SFN.

Materials and methods

Ethics statement and animal models

Use of TRAMP and Hi-Myc mice for the *in vivo* data presented herein was approved by the University of Pittsburgh–Institutional Animal Care and Use Committee. After transgene verification, 5-week-old male transgenic Hi-Myc mice (NIH mouse repository) were randomly divided into two groups. Control group of mice was administered with 100-µl corn oil, whereas the mice in the treatment group were administered with 1 mg SFN/mouse in 100-µl corn oil. Treatment was done by gavage three times per week for 5 weeks. At the end of the study, prostate tissues were collected and flash-frozen for *ex vivo* ^{1}H magnetic resonance spectroscopy or fixed in 10% neutral-buffered formalin for immunohistochemistry. Blood was collected at the time of sacrifice using heparin-coated syringe. Plasma was obtained after centrifuging the blood and stored at –80°C. Plasma and prostate/adenocarcinoma specimens from TRAMP mice from our previously published studies were used to determine the effect of SFN on markers of glycolysis (23,25).

Reagents

SFN (purity ≥ 98%) was purchased from LKT Laboratories (St. Paul, MN). Cell culture reagents were purchased from Life Technologies-Thermo Fisher Scientific (Waltham, MA) or Corning (Manassas, VA). Antibodies against phosphorylated s473 Akt, hexokinase II (HKII; for western blotting), pyruvate kinase M2 (PKM2) and LDHA (for western blotting) were purchased from Cell Signaling Technology (Danvers, MA); an antibody against β-actin was from Sigma–Aldrich (St. Louis, MO); a rabbit monoclonal anti-LDHA antibody used for immunofluorescence microscopy and immunohistochemistry was from Novus Biologicals (Centennial, CO); anti-glucose transporter (GLUT) 1 and anti-GLUT4 antibodies were purchased from Proteintech Group (Rosemont, IL), whereas anti-monocarboxylate transporter 1 (MCT1) antibody was purchased from Santa Cruz Biotechnology (Dallas, TX); and a rabbit polyclonal anti-HKII antibody used for immunofluorescence microscopy and immunohistochemistry was purchased from Abcam (Cambridge, MA). Kits for measurement of lactate (catalog #K607-100), pyruvate (catalog #K609-100), and glucose uptake (catalog #K676-100) were purchased from BioVision (Milpitas, CA).

Cell lines

The LNCaP, 22Rv1 and PC-3 cell lines were purchased from the American Type Culture Collection (Manassas, VA) and cultured by following supplier's recommendations. These cell lines were last authenticated by us in March 2017 and found to be of human origin and devoid of cross-contamination. The 22Rv1 cells stably transfected with empty pcDNA3 vector or pcDNA3-Myc plasmid were maintained as described by us previously (29). The 22Rv1 cells were stably transfected with empty pcDNA3 vector or

pcDNA3-myr-HA-Akt1 (constitutively active Akt, hereafter abbreviated as caAkt) plasmid and selected in the presence of 800 μg/ml of G418.

Determination of real-time extracellular acidification rate

The effect of SFN treatment on extracellular acidification rate (ECAR), a measure of glycolysis, in LNCaP, 22Rv1 or PC-3 cells was determined using the Seahorse Bioscience flux analyzer essentially as described by us previously (30). Briefly, 22Rv1 (3×10^4 cells per well) or PC-3 cells (1×10^4 cells per well) were plated in Seahorse XF96 cell culture microplates with three to six replicates. After overnight incubation, the cells were treated with dimethyl sulfoxide (DMSO) or SFN (5 or 10 μM) for 6 or 9 h. For LNCaP cells, Seahorse XF24 flux analyzer was used and the results were normalized for number of cells, while those from 22Rv1 and PC-3 cells were performed using Seahorse XF96 flux analyzer and normalized for crystal violet staining. Metabolic inhibitors like oligomycin (O), carbonyl cyanide-4-(trifluoromethoxy)phenylhydrazone (FCCP), rotenone (R), and 2-deoxyglucose (2-DG) were included as controls to ensure proper functioning of the Seahorse flux analyzer. The basal ECAR signifies acidification rate indicative of lactate production in the absence of metabolic inhibitors.

Immunofluorescence microscopy in cells

LNCaP (2×10^4) or 22Rv1 (3×10^4) cells were plated in triplicate on coverslips in 24-well plates. After overnight incubation, the cells were treated with DMSO or SFN (10 μM) for 24 h. The cells were then fixed and permeabilized with 2% paraformaldehyde and 0.5% Triton X-100, respectively. After blocking with phosphate-buffered saline containing 0.5% bovine serum albumin and 0.15% glycine, cells were treated overnight at 4°C with the desired primary antibody (HKII, PKM2 or LDHA) followed by Alexa Fluor 488-conjugated goat anti-rabbit antibody for 1 h, and then counterstained with DRAQ5 (nuclear stain) for 5 min at room temperature in the dark. Corrected total cell fluorescence was quantitated using ImageJ software.

Immunoblotting

Cells treated with DMSO (solvent control) or desired doses of SFN were lysed as described by us previously (31). Immunoblotting was performed as described by us previously (31). Blots were stripped and re-probed with anti-β-actin antibody for normalization. Immunoreactive bands were visualized by enhanced chemiluminescence method. Densitometric quantitation was performed with the use of UN-SCAN-IT version 5.1 (Silk Scientific Corporation, Orem, UT).

Immunohistochemistry

Immunohistochemistry was performed as described by us previously (26). Briefly, prostate tissues (Hi-Myc mice) or prostate adenocarcinoma (TRAMP mice) sections (4–5 μm thick) were de-paraffinized, hydrated in graded alcohol, and then washed with phosphate-buffered saline. Antigen retrieval was performed using citrate buffer solution (pH 6.0) at 100°C for 20 min. Sections were immersed in 0.3% hydrogen peroxide in 100% methanol for 20 min at room temperature. The tissue sections were incubated with the blocking buffer for 1 h followed by exposure to the desired primary antibody (HKII 1:50 dilution; PKM2 1:400 dilution; LDHA 1:50 dilution) in phosphate-buffered saline containing antibody diluting solution and background-reducing components (Dako; catalog #S3022) overnight in humid chambers at room temperature. Sections were treated with 3,3′-diaminobenzidine and counterstained with hematoxylin. At least 6–10 non-overlapping images were taken at ×40 objective magnification and analyzed by positive pixel count algorithm using Aperio ImageScope software.

Measurement of lactate and pyruvate levels

Lactate and/or pyruvate levels in cell lysate, plasma and tumor tissue supernatants from TRAMP mice, and in human plasma specimens were measured by using commercially available assay kits. Briefly, tumor tissues were sonicated in assay buffer. Tumor homogenates were centrifuged at 14 000 rpm for 10 min, and supernatant was used for protein estimation and lactate or pyruvate assay. Both supernatant from tumor homogenate and plasma were filtered using 10 kDa protein filter. Assays were performed according to the manufacturer's instructions.

Glucose uptake

LNCaP (1.5×10^5/well) or PC-3 (1×10^5/well) cells were plated in six-well plates in triplicate. Following overnight incubation, the cells were treated with DMSO or SFN (5 or 10 μM) for 24 h in complete growth medium. Cells were washed with glucose-free RPMI1640 medium, incubated in this medium for 40 min at 37°C in a 5% CO_2 incubator for glucose starvation, and further incubated for 20 min after adding 2 mM 2-DG to the cells. Instructions from the supplier of the kit were followed for glucose uptake assay.

Ex vivo ^{1}H magnetic resonance spectroscopy

Flash-frozen prostate tissue samples were placed into a 5-mm Shigemi NMR tube (Shigemi) with D_2O. Single voxel ^{1}H spectroscopy was performed at 500 MHz on a Bruker AVANCE 3HD 11.7 Tesla microimaging system equipped with a 5 mm MR microscopy RF resonator and ParaVision 6.0.1 (Bruker Biospin, Billerica, MA). Signal acquisition was carried out using a point-resolved spectroscopy sequence (32) with VAPOR water suppression (33) from a $2 \times 2 \times 2\,mm^3$ voxel placed in the center of the sample. The protocol parameters were as follows: TR/TE = 2500/30 ms, spectral bandwidth = 10 kHz, number of data points = 2,048, number of averages = 256. Localized shimming was performed with Mapshim, yielding a water line width of ~15 Hz. The 1D proton spectra were analyzed using Topspin 3.1 software (Bruker Biospin, Billerica, MA). The signal intensity was determined from spectral peaks of lactate (4.2 p.p.m., Lac), myo-inositol (3.7 p.p.m., MI), taurine (3.4 p.p.m., Tau), creatine (3.0 p.p.m., Cr), citrate (2.6 p.p.m., Cit) and polyamines (1.9 p.p.m.). Results are expressed as the following metabolite ratios: Lac/Cr, MI/Cr, Tau/Cr and Cit/Cr.

Clonogenic assay

22Rv1 (1000 cells) cells overexpressing Myc or caAkt and corresponding empty vector-transfected control cells were seeded in six-well plates in triplicate and allowed to attach by overnight incubation. Cells were treated with DMSO or desired doses of SFN. The medium containing DMSO or SFN was replaced every third day. After 8 days of treatment, cells were fixed with 100% methanol for 5 min at room temperature and stained with 0.5% crystal violet solution in 20% methanol for 30 min at room temperature.

Clinical specimens

Plasma specimens from a previously published clinical study of SFN-BSE in prostate cancer patients with biochemical recurrence were used for the measurement of lactate and pyruvate levels (20). This study was conducted at the Knight Cancer Institute, Oregon Health and Science University (Joshi J. Alumkal, Principal Investigator), and was registered at the clinicaltrials.gov (NCT01228084). Details of the study design, patient population and characteristics, and treatment can be found in Alumkal *et al.* (20).

Statistical analyses

Statistical significance of difference was determined by Student's *t*-test or one-way analysis of variance (ANOVA) followed by Dunnett's adjustment (dose–response) or Bonferroni's (multiple comparison) test using GraphPad Prism (version 7.02).

Results

SFN treatment decreased ECAR in cultured LNCaP and 22Rv1 human prostate cancer cells

Initially, we explored the possibility of whether SFN treatment inhibited ECAR, a measure of glycolysis rate, in LNCaP and 22Rv1 cells following 6 or 9 h treatment with 5 and 10 μM SFN. LNCaP and 22Rv1 cells were selected because they are well-characterized representatives of androgen-responsive and

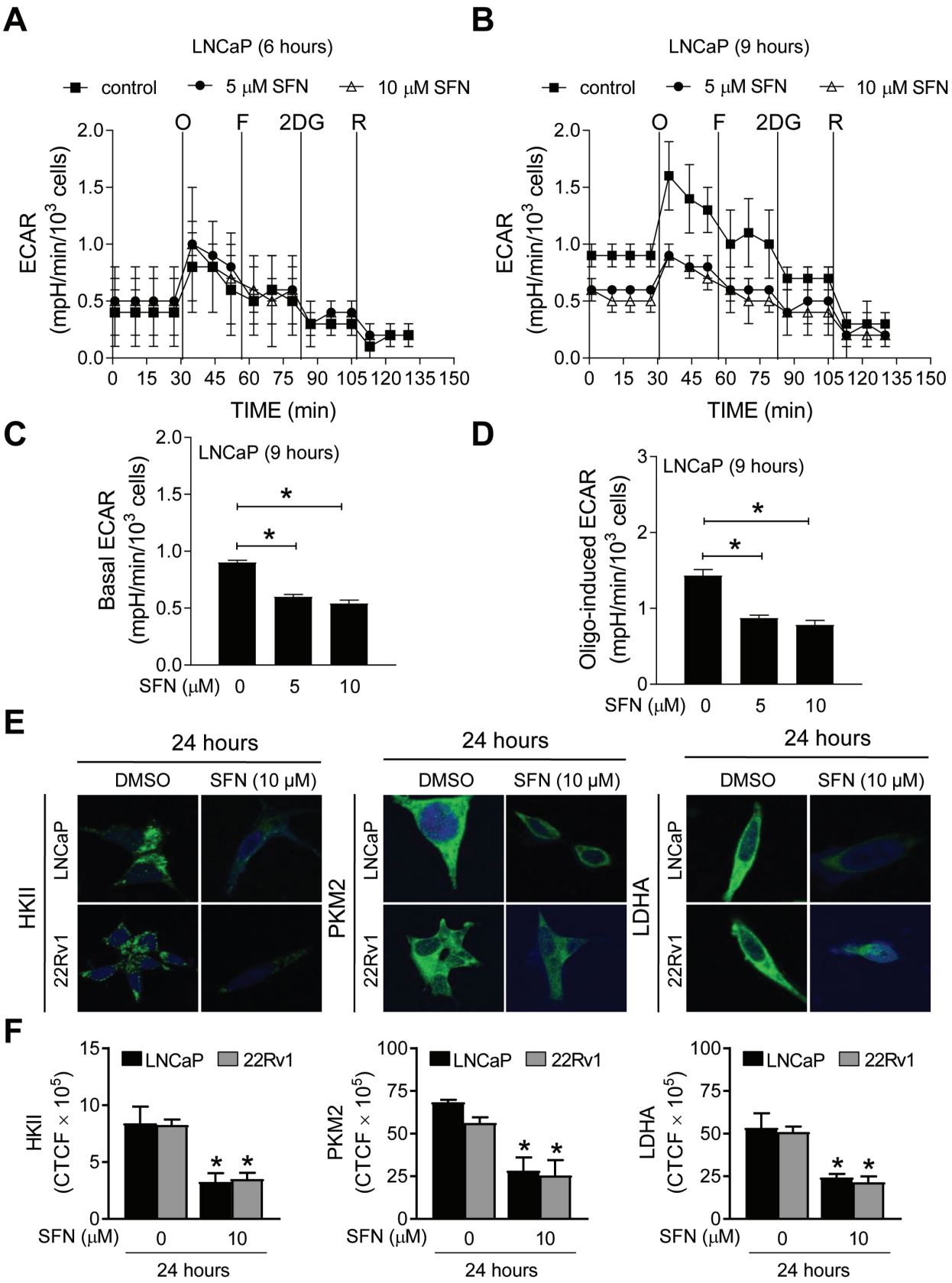

Figure 1. SFN treatment decreased ECAR and protein levels of HKII, PKM2 and LDHA in prostate cancer cells. Pharmacologic profiling of ECAR in LNCaP cells through real-time measurements using the Seahorse flux analyzer following 6- (**A**) or 9-h (**B**) treatment with DMSO or SFN (5 or 10 μM). After measurement of basal ECAR, the cells were treated with metabolic inhibitors, including 1 μM oligomycin (O), 300 nM carbonyl cyanide-4-(trifluoromethoxy)phenylhydrazone (FCCP) (F), 1 mM 2-deoxy glucose (2-DG) or 1 μM rotenone (R) at the indicated times. Basal ECAR was calculated using the difference between the mean of time points prior to injection of O (#1 to #4). Oligomycin-sensitive rate was calculated using the difference between the mean of time points prior to injection of F (#5 to #7). Quantitation of basal ECAR (**C**)

castration-resistant prostate cancer cells. A highly glycolytic cell line that lacks AR expression (PC-3) (14) was also included for comparison. The doses for SFN for the *in vitro* studies were selected based on the results of our own clinical trial with SFN-BSE in patients with atypical nevi (34). The plasma levels of SFN reached up to 7.4 μM (range: 2.2–7.4 μM) after 28 days of daily oral treatment with 200 μmol BSE-SFN (34). Real-time ECAR in LNCaP cells following 6- and 9-h treatment with DMSO (solvent control) or 5 and 10 μM SFN are shown in Figure 1A and B, respectively. The basal ECAR (Figure 1C) in the absence of metabolic inhibitors and oligomycin-induced ECAR (Figure 1D) were significantly lower in SFN-treated LNCaP cells when compared with the solvent control. The effect of SFN on ECAR was inconsistent in 22Rv1 cells (data not shown). On the other hand, PC-3 cell line was resistant to ECAR inhibition by SFN treatment in three independent experiments (Supplementary Figure S1A–C, available at *Carcinogenesis* online). These results indicated suppression of ECAR by SFN treatment in LNCaP cells but not in a highly glycolytic cell line (PC-3).

SFN treatment downregulated expression of HKII, PKM2 and LDHA in LNCaP and 22Rv1 human prostate cancer cell lines *in vitro*

Lactate production in glycolysis starts with glucose uptake and is facilitated by a series of catalytic steps. We determined the effect of SFN treatment on protein levels of several glycolysis-related enzymes, including HKII, PKM2 and LDHA, that are overexpressed in prostate cancer (15,35). Figure 1E depicts immunocytochemical staining for HKII, PKM2 and LDHA in LNCaP and 22Rv1 cells treated for 24 h with DMSO or 10 μM SFN. Each protein was primarily localized in the cytoplasm in DMSO-treated control LNCaP and 22Rv1 cells (Figure 1E). The cytoplasmic levels of HKII, PKM2 and LDHA proteins were lower following SFN treatment in both cell lines (Figure 1F). Because ECAR was not inhibited by SFN treatment in PC-3 cells, this cell line was not included in this experiment. The results of immunofluorescence microscopy were confirmed by western blotting revealing downregulation of HKII, PKM2 and LDHA in SFN-treated LNCaP and 22Rv1 cells (Figure 2A).

SFN administration decreased tumor expression of glycolysis-related proteins and plasma lactate level in TRAMP mice *in vivo*

We have shown previously that oral SFN administration (three times per week for 17–19 weeks) prevents prostate cancer development in TRAMP mice (23). In this study, the incidence of PIN and well-differentiated adenocarcinoma in the dorsolateral prostate was lower by ~23–28% in the SFN treatment group compared with controls (23). SFN administration also caused a decrease in area of well-differentiated adenocarcinoma compared with the control group (23). Prostate adenocarcinoma sections from control and SFN-treated TRAMP mice were used to determine expression of HKII, PKM2 and LDHA. Immunohistochemistry images for glycolysis-related enzyme proteins in the prostate adenocarcinoma of control and SFN-treated TRAMP mice are shown in Figure 2B. The prostate tumor expression of HKII, PKM2 and LDHA proteins was decreased by 32–45% (HKII: 32%; PKM2: 45%; LDHA: 33%) in the SFN treatment group compared with control, and the difference was statistically significant for PKM2 (Figure 2C). Furthermore, oral SFN administration resulted in a significant decrease in both plasma and prostate tumor levels of lactate in comparison with control mice (Figure 3A).

SFN administration decreased lactate level in the prostate of Hi-Myc mice

We used Hi-Myc mice to further test the inhibitory effect of SFN administration on glycolysis. Unlike TRAMP mice, this study was not powered to determine the effect of SFN treatment on incidence of PIN and invasive carcinoma. Figure 3B shows ^{1}H magnetic resonance signals for various metabolites, including Lac, MI, Tau, Cit and polyamines, in the prostate of a control Hi-Myc mouse. Five-week treatment of Hi-Myc mice with SFN (1 mg/mouse, three times per week—this dose is comparable with that used in the TRAMP mice; ref. 23) starting at 5 weeks of age (10 weeks of age at sacrifice) resulted in a statistically significant decrease in the Lac/Cr signal ratio when compared with control mice (Figure 3C; $n = 6$ for control and $n = 5$ for SFN group). The signal ratio was very weak in one specimen from the SFN treatment group that was not included in the data analysis. The Hi-Myc mice at 10 weeks of age predominantly develop PIN lesions. The expression of HKII, PKM2 and LDHA protein was statistically significantly lower in the PIN lesions of SFN-treated mice when compared with control as revealed by immunohistochemistry (Figure 4). Collectively, these results provided *in vivo* evidence for SFN-mediated suppression of glycolysis in prostate cancer cells.

Effect of SFN treatment on glucose uptake

We also considered the possibility of whether SFN-mediated decrease in glycolysis was due to inhibition of glucose uptake. As shown in Supplementary Figure S2 (available at *Carcinogenesis* online), glucose uptake was modestly but significantly decreased by SFN treatment in LNCaP cells at the 10 μM concentration. On the other hand, SFN treatment caused an increase in glucose uptake in PC-3 cells (Supplementary Figure S2, available at *Carcinogenesis* online), which may be due to an increase in GLUT1 expression in this cell line (Supplementary Figure S3A and B, available at *Carcinogenesis* online). The western blotting for GLUT1, GLUT4 and MCT1 proteins was repeated three times using independently prepared lysates from control and SFN-treated LNCaP and PC-3 cells (Supplementary Figure S3A, available at *Carcinogenesis* online). Probing with the anti-GLUT1 and anti-GLUT4 antibodies exhibited nonspecific band(s) in each experiment for the PC-3 cells. However, densitometric quantitation was done for the correct molecular weight size band for each protein. The expression of GLUT1, GLUT4 and MCT1 was not significantly altered by SFN treatment in LNCaP cells as evidenced by densitometric quantitation of western blots.

Myc overexpression partially attenuated SFN-mediated suppression of glycolysis

Next, we investigated the mechanism underlying glycolysis inhibition by SFN using cultured prostate cancer cells. We

and oligomycin-sensitive ECAR (**D**) in LNCaP cells following 9-h treatment with DMSO or SFN. Quantitative data for the 6-h time point are not shown as the difference was not significant. The experiment was repeated three times in triplicate, and combined data are expressed as mean ± SEM. Significantly different (*$P < 0.05$) compared with control by one-way ANOVA followed by Dunnett's test. (**E**) Confocal images (×63 oil objective magnification) for HKII, PKM2 and LDHA (green fluorescence) in LNCaP and 22Rv1 cells following 24-h treatment with DMSO or 10 μM SFN. Nucleus was stained with DRAQ5 (blue fluorescence). (**F**) Quantitation of corrected total cell fluorescence (CTCF) using ImageJ software in LNCaP and 22Rv1 cells following treatment with DMSO or SFN for the specified time points. *Significant ($P < 0.05$) compared with DMSO-treated control by Student's *t*-test. Results were consistent in two independent experiments.

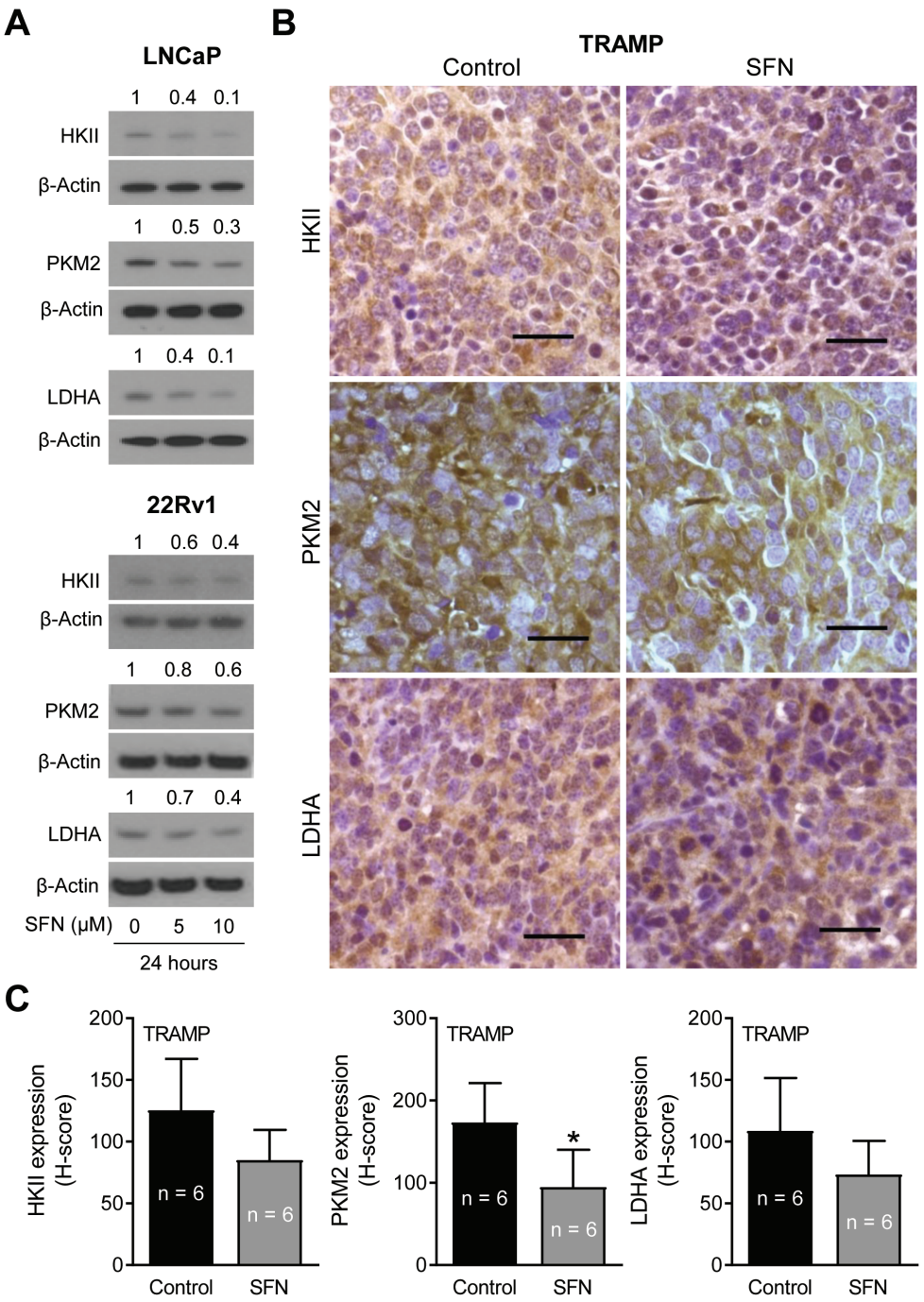

Figure 2. SFN treatment inhibited expression of glycolysis-related enzyme proteins in prostate cancer cells *in vitro* and *in vivo*. (**A**) Immunoblotting for HKII, PKM2 and LDHA proteins using lysates from LNCaP and 22Rv1 cells after 24-h treatment with DMSO or the indicated doses of SFN. Numbers above bands are fold changes in protein expression relative to respective DMSO-treated controls. (**B**) Immunohistochemical images for HKII, PKM2 and LDHA protein expression in representative prostate adenocarcinoma sections of TRAMP mice (×40 objective magnification, scale bar = 50 μm). (**C**) H-score for HKII, PKM2 and LDHA protein expression in TRAMP tumor section. The results shown are mean ± SD ($n = 6$). Statistical analysis was performed by Student's *t*-test (*$P < 0.05$).

focused on Myc and Akt because they both have been implicated in regulation of glycolysis (13,36). Overexpression of Myc and caAkt in stably transfected 22Rv1 cells was confirmed by western blotting (Figure 5A). SFN-mediated downregulation of HKII, PKM2 and LDHA was markedly attenuated by overexpression of Myc, but not caAkt (Figure 5B). As an example, the protein expression of LDHA in empty vector-transfected control 22Rv1 cells was decreased by ~80% upon 24-h treatment with 10 μM SFN in comparison with solvent-treated control cells. A similar SFN treatment caused only ~30% decrease in LDHA protein expression in Myc overexpressing cells (Figure 5B). Clonogenic survival of empty vector-transfected control 22Rv1 cells was dose dependently inhibited in the presence of SFN, and this effect was partially attenuated by overexpression of Myc, but not caAkt (Figure 5C and D). Finally, overexpression of Myc, but not caAkt, conferred protection against decrease in intracellular lactate levels resulting from SFN treatment (Figure 5E).

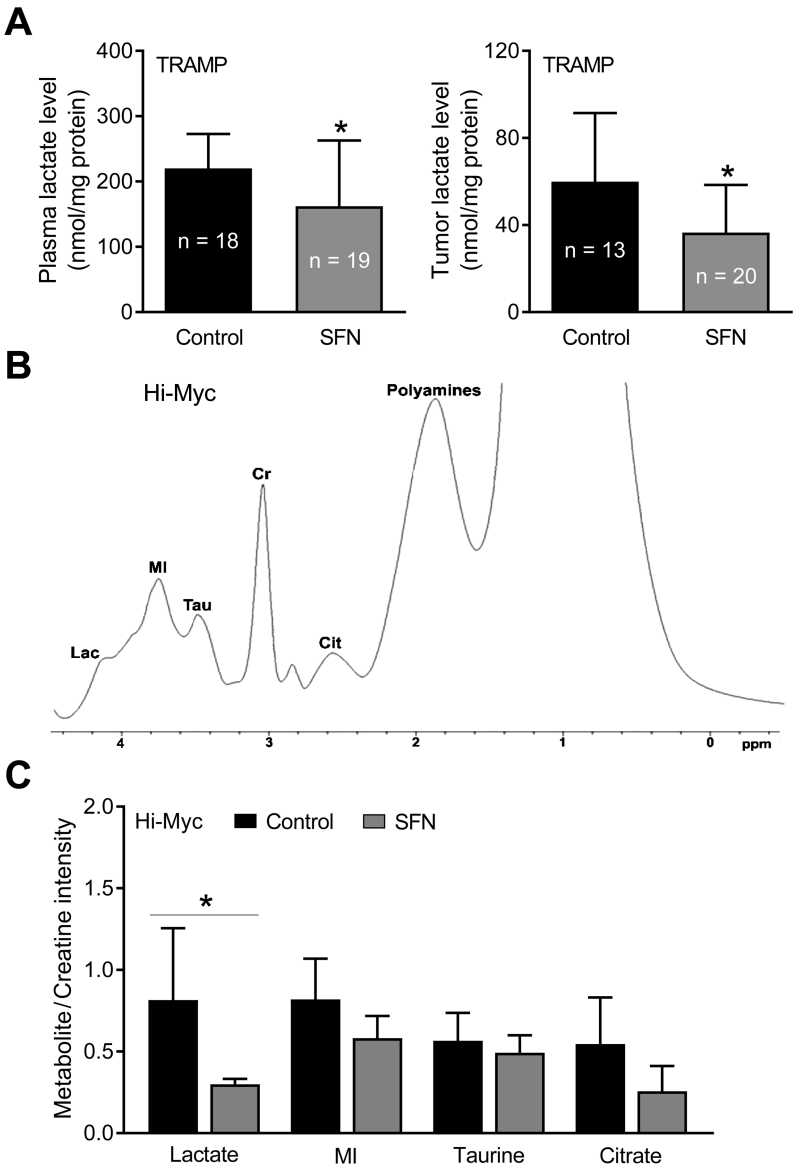

Figure 3. SFN administration decreased lactate levels in the plasma and prostate adenocarcinoma of TRAMP mice *in vivo*. (**A**) Lactate levels in the plasma and prostate tumors of control and SFN-treated TRAMP mice. Results shown are mean ± SD (n = 18–19 for plasma and n = 13–20 for tumors). Plasma and tumor samples from different mice of each group were used for the assay. Statistical significance was determined by Student's t-test (*$P < 0.05$). (**B**) Representative *ex vivo* ^{1}H magnetic resonance spectrum of different metabolites in the prostate of a control Hi-Myc mouse. (**C**) Quantitation of the metabolite levels in the prostate of Hi-Myc mice. The results shown are mean ± SD (n = 6 for control group and n = 5 for SFN treatment group). Statistical significance was determined by Student's t-test (*$P < 0.05$).

Oral SFN-BSE administration did not decrease circulating levels of lactate in humans

Plasma specimens collected at baseline and 9, 17 and 21 weeks after SFN-BSE treatment were used to measure lactate and pyruvate levels. SFN-BSE administration did not lower circulating levels of lactate (Figure 6A) or pyruvate (Figure 6B) even after 21 weeks of administration. However, additional clinical studies are needed to determine whether SFN administration can alter prostate tumor levels of lactate.

Discussion

The present study provides *in vitro* and *in vivo* evidence for reversal of the Warburg effect in prostate cancer by a phytochemical that is safe and exhibits preventative activity in preclinical models of prostate cancer (23,25). The glycolysis inhibition by SFN is associated with a significant decrease in protein levels of key enzymes, including HKII, PKM2 and LDHA, at least in the Hi-Myc mouse model. A trend for reduced expression of these proteins was also discernible in prostate adenocarcinoma of TRAMP mice, although the difference from controls was not significant for HKII and LDHA due to a large variability. Published studies have shown alterations in expression of these proteins in prostate cancer (15,37). The expression of HKII, which catalyzes the first step in glucose metabolism by converting it to glucose-6-phosphate, is significantly higher in prostate cancers, especially castration-resistant disease, in comparison with benign prostate hyperplasia (37). The expression of HKII is increased following androgen deprivation in *Pten/Tp53*-deficient prostate cancer models (38). Studies have also established that HKII-mediated glycolysis is required for *Pten*- and *p53*-deficiency-driven prostate

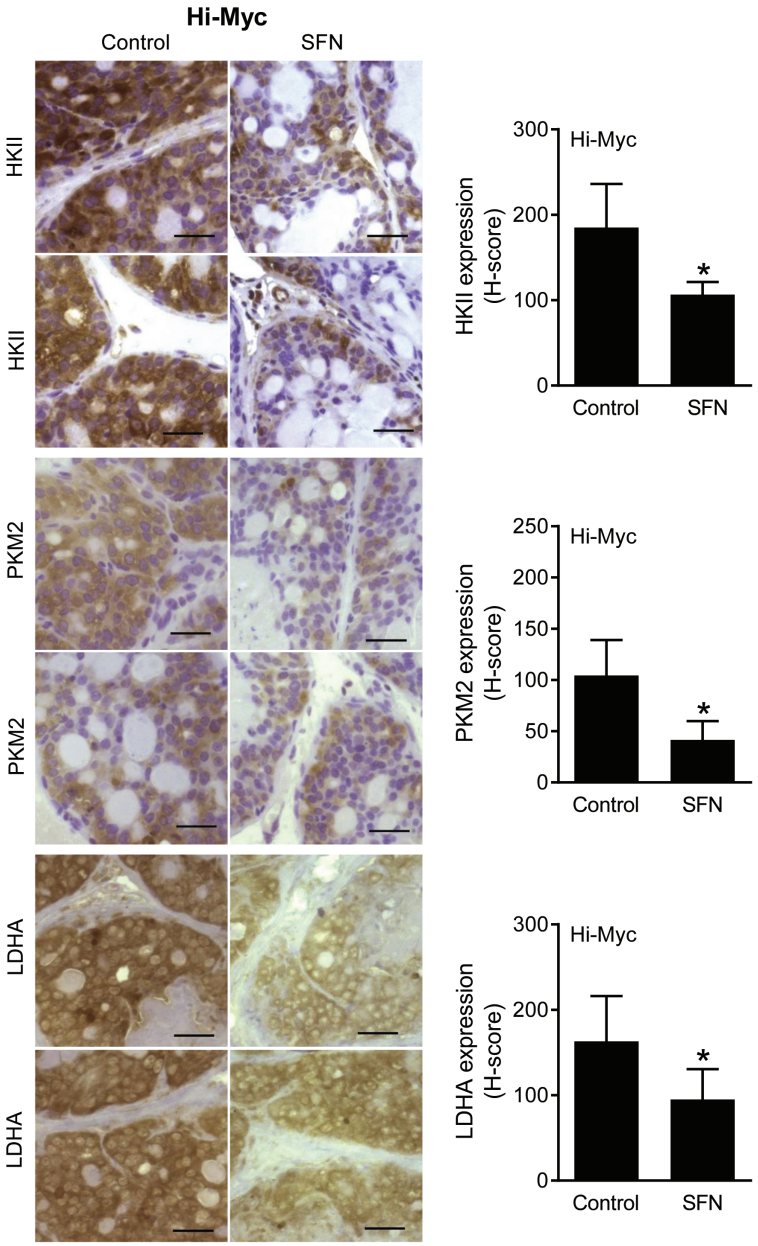

Figure 4. SFN treatment downregulated expression of glycolysis-related proteins in PIN lesions of Hi-Myc mice. Immunohistochemical images for HKII, PKM2 and LDHA protein expression in representative prostate sections of control and SFN-treated Hi-Myc mice (×40 objective magnification, scale bar = 50 μm) are shown in the left panel. Quantitative data for H-score are shown are mean ± SD ($n = 5$) in the right panel. Statistical analysis was performed by Student's *t*-test (*$P < 0.05$).

cancer (39). Similarly, immunohistochemistry revealed high expression of PKM2 protein, which is responsible for the conversion of phosphoenolpyruvate to pyruvate, in high Gleason grade tumors (35). A significant positive association between nuclear expression of PKM2 with aggressiveness has also been observed in prostate cancer (40). As mentioned previously, expression of LDHA, which catalyzes the conversion of pyruvate to lactate, is also higher in prostate cancer specimens when compared with benign prostate hyperplasia (15). Taken together, data presented herein suggest that circulating levels of lactate coupled with tumor expression of HKII, PKM2 and LDHA may be useful biomarkers of SFN or SFN-BSE in future clinical trials. Identification of mechanistic biomarkers is essential especially for the clinical development of cancer chemopreventive interventions. Other mechanistic effects of SFN in prostate cancer cells are summarized in Figure 6C (22,23,25–27,41,42).

SFN treatment was unable to inhibit ECAR in PC-3 cells, which lack AR expression. These results suggest that anti-glycolytic effect of SFN in prostate cancer cells may be AR dependent. In this context, we have shown previously that SFN treatment inhibits activity of AR and Myc in prostate cancer cells (27,42). Studies have also implicated AR in upregulation of Myc expression (43).

It is interesting to note that SFN administration suppresses fatty acid synthesis (26) as well as glycolysis (present study) in the TRAMP mouse model. These observations raise the question of whether these mechanistic effects of SFN are interrelated. Acetyl-CoA, which is the building block of fatty acid synthesis, is partly generated by pyruvate dehydrogenase complex-mediated decarboxylation of glycolysis intermediate pyruvate. We have shown previously that SFN administration decreases plasma and prostate tumor levels of acetyl-CoA in TRAMP mice (26). Therefore, it is reasonable to postulate that

Figure 5

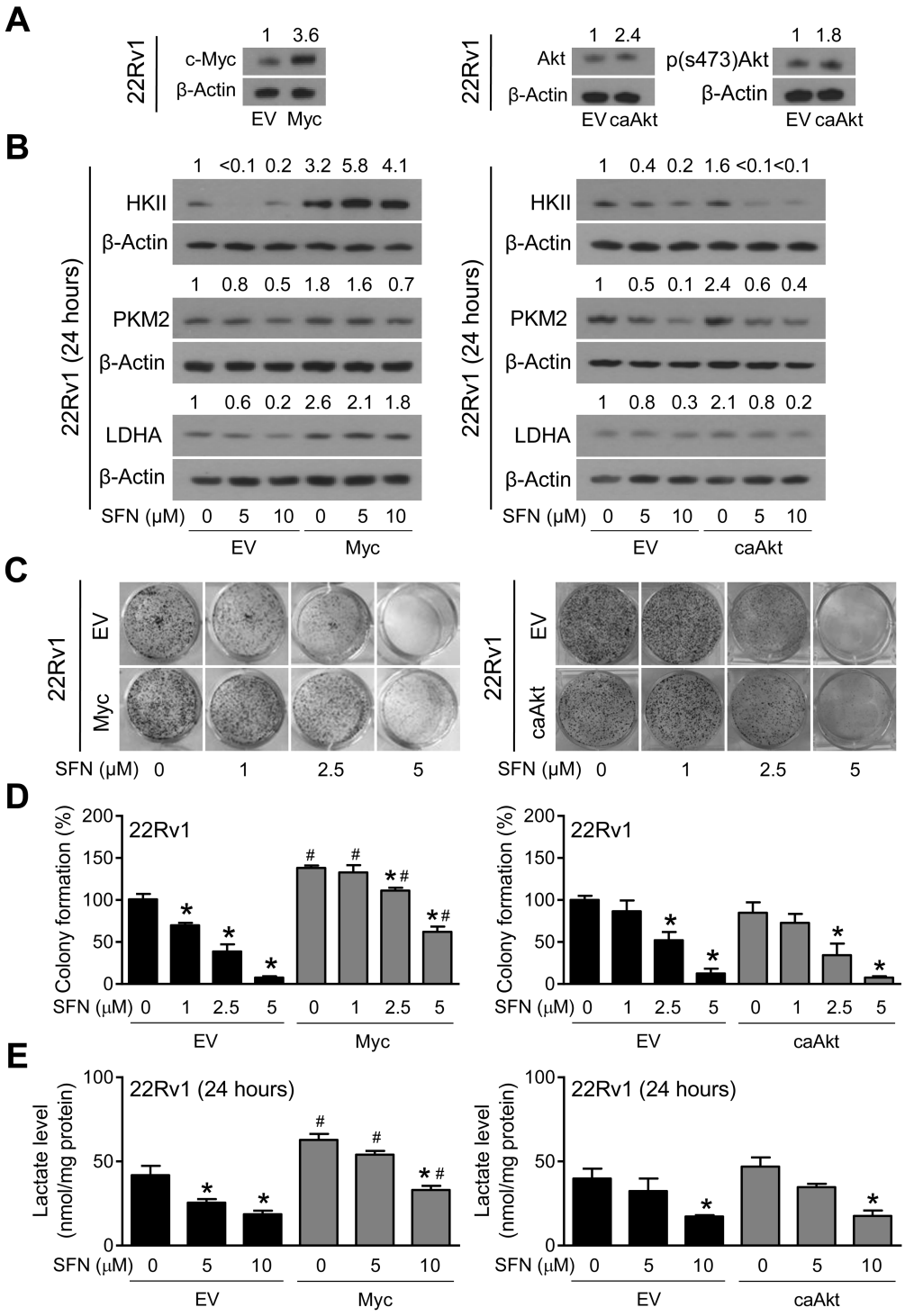

Figure 5. Overexpression of Myc, but not constitutively active Akt (caAkt) partially attenuated SFN-mediated decrease in protein levels of HKII, PKM2, and LDHA in 22Rv1 cells. (**A**) Immunoblotting for Myc, total Akt, and phosphorylated s473 Akt using lysates from 22Rv1 cells stably transfected with empty vector, Myc or caAkt. (**B**) Immunoblotting for HKII, PKM2 and LDHA using lysates from 22Rv1 cells stably transfected with empty vector (EV) or Myc or caAkt plasmids and treated for 24 h with DMSO or the indicated doses of SFN. (**C**) Representative images of colonies resulting from 22Rv1 cells after 8 days of treatment with DMSO or the indicated doses of SFN. (**D**) Quantitation of colony formation. Results shown are mean ± SD ($n = 3$). Statistically significant ($P < 0.05$) compared with the *corresponding DMSO-treated control or #between cells transfected with EV and Myc or caAkt by one-way ANOVA followed by Bonferroni's multiple comparisons test. Comparable results were obtained from replicate experiments. (**E**) Intracellular lactate levels in 22Rv1 cells stably transfected with EV or Myc or caAkt plasmids and treated for 24 h with DMSO or the indicated doses of SFN. Results shown are mean ± SD ($n = 3$). Statistically significant ($P < 0.05$) compared with the *corresponding DMSO-treated control or #between cells transfected with EV and Myc or caAkt by one-way ANOVA followed by Bonferroni's multiple comparisons test. Each experiment was repeated at least two times.

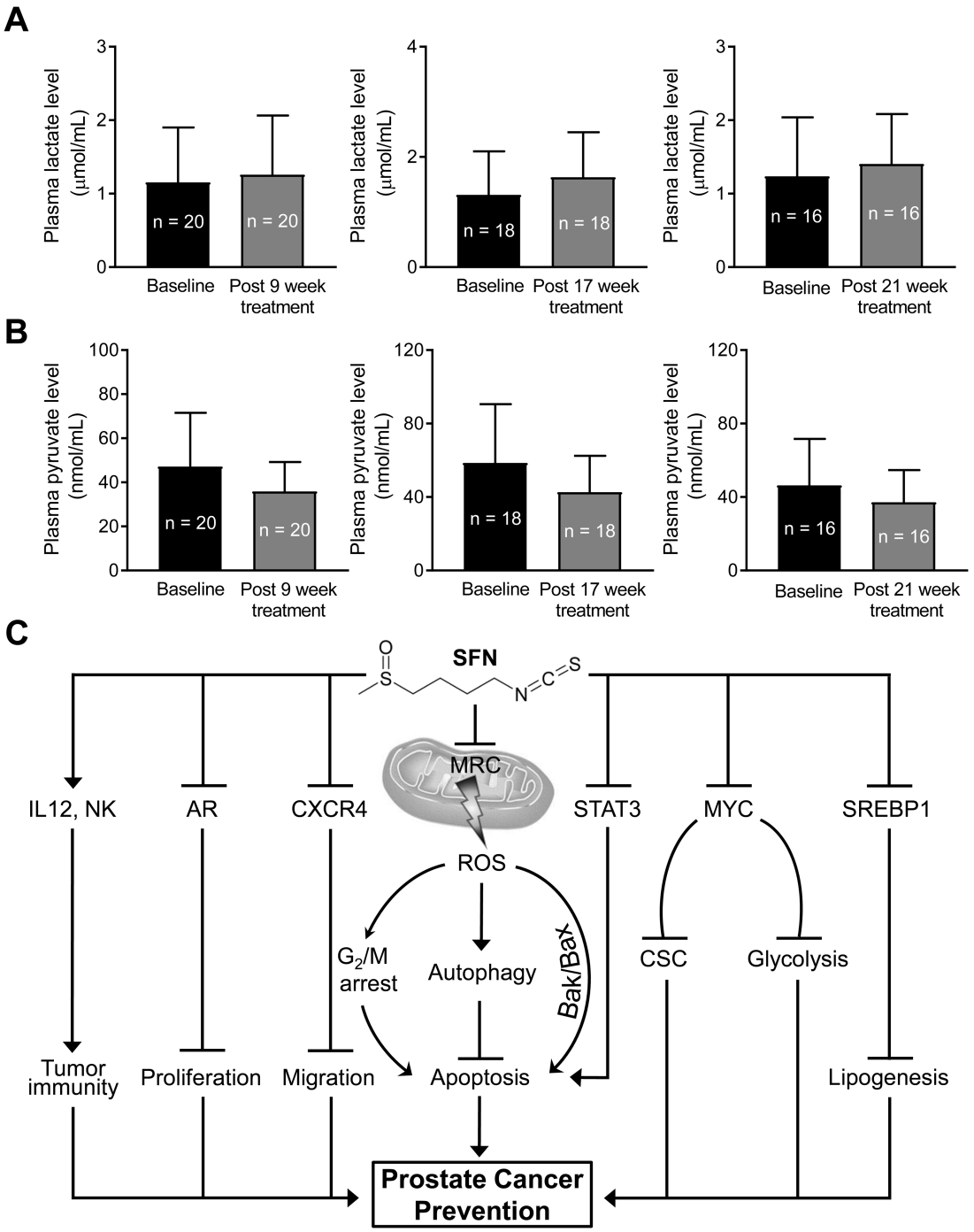

Figure 6. SFN-BSE administration did not alter plasma levels of lactate or pyruvate in a clinical study. Basal and post-SFN-BSE treatment plasma levels of lactate (**A**) and pyruvate (**B**). (**C**) A cartoon summarizing mechanistic effects of SFN in prostate cancer cells (22,23,25–27,41,42).

acetyl-CoA suppression is probably the common mechanistic link in SFN-mediated inhibition of fatty acid synthesis (26) and glycolysis (present study).

Studies have indicated a role for Myc as well as Akt not only in the regulation of glycolysis but also in the pathogenesis of human prostate cancer (28,44,45). The expression of *c-Myc* is positively associated with that of *HKII* and *LDHA*, but not *PKM2*, in prostate cancer TCGA (46). Both these oncogenic regulators are inhibited by SFN or SFN-BSE treatment in prostate cancer cells *in vitro* and/or in TRAMP tumors *in vivo* (24,47). Overexpression of Myc attenuates the inhibitory effect of SFN on prostate cancer stem-like cells (27). The present study also reveals attenuation of SFN-mediated inhibition of glycolysis by overexpression of Myc, but not by overexpression of caAkt. Partial reversal of glycolysis inhibition by SFN after Myc overexpression suggests that additional mechanism(s) are probably contributing to the glycolysis inhibition by SFN. For example, studies have implicated histone methyltransferase enhancer of zeste homolog 2 (EZH2)/micro RNA miR-181b axis in regulation of HKII and glycolysis (37). Increased glycolysis is reported following overexpression of

both full-length AR and its splice variant AR-V7, the latter is robustly expressed in 22Rv1 cells (48). SFN is known to inhibit AR as well as AR-V7 in 22Rv1 cells (42,49). This is significant because the presence of AR-V7 splice variant in the circulating tumor cells in metastatic castration-resistant prostate cancer patients was associated with primary resistance to enzalutamide and abiraterone. The effect of SFN on EZH2 is yet to be studied in prostate cancer cells, but it is possible that inhibition of glycolysis by this phytochemical may also be regulated by EZH2 and/or AR signaling axis. Studies are necessary to systematically explore these alternate mechanistic possibilities in glycolysis inhibition by SFN.

Inhibition of glycolysis appears to be a common metabolic effect for at least two different isothiocyanates, including phenethyl isothiocyanate (46) and SFN (present study). Like antiglycolytic effects of SFN showed in the present study, phenethyl isothiocyanate treatment also suppresses protein levels of HKII, PKM2 and LDHA in cultured LNCaP and 22Rv1 prostate cancer cells *in vitro* and decreases plasma lactate levels in TRAMP mice *in vivo* (46). Consistent with the results of the present study, colony formation inhibition; suppression of HKII, PKM2 and LDHA protein expression; and decrease in intracellular levels of lactate resulting from treatment with phenyl isothiocyanate are partly attenuated by overexpression of Myc at least in 22Rv1 cells (46).

A few studies have documented conflicting effects of SFN on immune cells (reviewed in ref. (50). The authors of this review article suggested that SFN may interfere with T cell-mediated cancer immunotherapies (50). Further studies are needed for experimental validation of this concern, but we have shown previously that prostate cancer prevention by SFN in TRAMP mice is accompanied by increased activity of natural killer cells (23).

Studies have clinically investigated SFN-BSE and stabilized free SFN for their effects on AR activity (20,21). In one study of SFN-BSE in 20 prostate cancer patients with biochemical recurrence characterized by rising prostate-specific antigen (PSA) levels, the primary end point of ≥50% decline in the PSA was observed in only one patient, but there were no Grade 3 or 4 adverse events in any subject. Several patients exhibited a smaller decrease in PSA level (20). Interestingly, a significant lengthening of the on-treatment PSA doubling time was observed when compared with the pretreatment doubling time (20). In a double-blinded, randomized, placebo-controlled multicenter trial in prostate cancer patients with biochemical recurrence, a consistent decrease in median log PSA slopes was observed by daily oral administration of 60 mg of stabilized free sulforaphane for 6 months (21). However, the primary end point of 0.012 log (ng/ml) PSA/month decrease was not observed (21). This study also reported an 86% longer PSA doubling time in the SFN treatment group when compared with patients receiving a placebo (21).

In the present study, analysis of the plasma specimens from one of these studies (20) did not indicate a decrease in lactate levels. Several possibilities exist to explain these negative results. First, we still do not know if the prostate adenocarcinoma level of lactate is affected by treatment with SFN-BSE or free SFN. Second, in all cases, subjects enrolled in the clinical trial consumed their last dose of SFN-BSE the day prior to blood collection (20). Thus, we do not know the effect of SFN-BSE on lactate at time points closer to dosing. Third, treatment duration longer than 21 weeks or a higher dose of SFN-BSE or SFN may be necessary for decreasing circulating levels of lactate.

In conclusion, the present study demonstrates that a very mild regimen of three times per week SFN administration significantly decreases lactate levels in the plasma and prostate of Hi-Myc and TRAMP mice. Inhibition of Myc-regulated expression of HKII and LDHA is partially responsible for reversal of the Warburg effect by SFN. However, additional clinical studies are necessary to determine whether SFN or SFN-BSE administration can suppress prostate tumor levels of lactate or expression of HKII, PKM2 and/or LDHA.

Supplementary material

Supplementary data are available at *Carcinogenesis* online.

Funding

This study was supported in part by the National Cancer Institute grants RO1 CA225716-01A1 and CA101753-14 (S.V.S., Principal Investigator) and Kuni Foundation Clinical Trial Award (J.J.A., Principal Investigator).

Acknowledgements

This study used the UPMC Hillman Cancer Center Core Facilities, including the Animal Facility, the Tissue and Research Pathology Facility, and the *In Vivo* Imaging Facility, supported in part by the National Cancer Institute grant P30 CA047904 (R.L.F., Principal Investigator).
Conflict of Interest Statement: None declared.

References

1. Siegel, R.L. *et al.* (2018) Cancer statistics, 2018. *CA. Cancer J. Clin.*, 68, 7–30.
2. Hanahan, D. *et al.* (2011) Hallmarks of cancer: the next generation. *Cell*, 144, 646–674.
3. Zadra, G. *et al.* (2013) The fat side of prostate cancer. *Biochim. Biophys. Acta*, 1831, 1518–1532.
4. Liu, Y. (2006) Fatty acid oxidation is a dominant bioenergetic pathway in prostate cancer. *Prostate Cancer Prostatic Dis.*, 9, 230–234.
5. Rossi, S. *et al.* (2003) Fatty acid synthase expression defines distinct molecular signatures in prostate cancer. *Mol. Cancer Res.*, 1, 707–715.
6. Migita, T. *et al.* (2009) Fatty acid synthase: a metabolic enzyme and candidate oncogene in prostate cancer. *J. Natl Cancer Inst.*, 101, 519–532.
7. De Schrijver, E. *et al.* (2003) RNA interference-mediated silencing of the fatty acid synthase gene attenuates growth and induces morphological changes and apoptosis of LNCaP prostate cancer cells. *Cancer Res.*, 63, 3799–3804.
8. Brusselmans, K. *et al.* (2005) RNA interference-mediated silencing of the acetyl-CoA-carboxylase-alpha gene induces growth inhibition and apoptosis of prostate cancer cells. *Cancer Res.*, 65, 6719–6725.
9. Gao, Y. *et al.* (2014) Inactivation of ATP citrate lyase by Cucurbitacin B: a bioactive compound from cucumber, inhibits prostate cancer growth. *Cancer Lett.*, 349, 15–25.
10. Angeles, T.S. *et al.* (2016) Recent advances in targeting the fatty acid biosynthetic pathway using fatty acid synthase inhibitors. *Expert Opin. Drug Discov.*, 11, 1187–1199.
11. Tessem, M.B. *et al.* (2008) Evaluation of lactate and alanine as metabolic biomarkers of prostate cancer using ^{1}H HR-MAS spectroscopy of biopsy tissues. *Magn. Reson. Med.*, 60, 510–516.
12. Keshari, K.R. *et al.* (2013) Metabolic reprogramming and validation of hyperpolarized ^{13}C lactate as a prostate cancer biomarker using a human prostate tissue slice culture bioreactor. *Prostate*, 73, 1171–1181.
13. Priolo, C. *et al.* (2014) AKT1 and MYC induce distinctive metabolic fingerprints in human prostate cancer. *Cancer Res.*, 74, 7198–7204.
14. Pertega-Gomes, N. *et al.* (2015) A glycolytic phenotype is associated with prostate cancer progression and aggressiveness: a role for monocarboxylate transporters as metabolic targets for therapy. *J. Pathol.*, 236, 517–530.
15. Xian, Z.Y. *et al.* (2015) Inhibition of LDHA suppresses tumor progression in prostate cancer. *Tumour Biol.*, 36, 8093–8100.

16. WARBURG, O. (1956) On the origin of cancer cells. *Science*, 123, 309–314.
17. Semenza, G.L. (2008) Tumor metabolism: cancer cells give and take lactate. *J. Clin. Invest.*, 118, 3835–3837.
18. Vander Heiden, M.G. *et al.* (2009) Understanding the Warburg effect: the metabolic requirements of cell proliferation. *Science*, 324, 1029–1033.
19. Sborov, D.W. *et al.* (2015) Investigational cancer drugs targeting cell metabolism in clinical development. *Expert Opin. Investig. Drugs*, 24, 79–94.
20. Alumkal, J.J. *et al.* (2015) A phase II study of sulforaphane-rich broccoli sprout extracts in men with recurrent prostate cancer. *Invest. New Drugs*, 33, 480–489.
21. Cipolla, B.G. *et al.* (2015) Effect of sulforaphane in men with biochemical recurrence after radical prostatectomy. *Cancer Prev. Res. (Phila.)*, 8, 712–719.
22. Singh, A.V. *et al.* (2004) Sulforaphane induces caspase-mediated apoptosis in cultured PC-3 human prostate cancer cells and retards growth of PC-3 xenografts *in vivo*. *Carcinogenesis*, 25, 83–90.
23. Singh, S.V. *et al.* (2009) Sulforaphane inhibits prostate carcinogenesis and pulmonary metastasis in TRAMP mice in association with increased cytotoxicity of natural killer cells. *Cancer Res.*, 69, 2117–2125.
24. Keum, Y.S. *et al.* (2009) Pharmacokinetics and pharmacodynamics of broccoli sprouts on the suppression of prostate cancer in transgenic adenocarcinoma of mouse prostate (TRAMP) mice: implication of induction of Nrf2, HO-1 and apoptosis and the suppression of Akt-dependent kinase pathway. *Pharm. Res.*, 26, 2324–2331.
25. Vyas, A.R. *et al.* (2013) Chemoprevention of prostate cancer by D,L-sulforaphane is augmented by pharmacological inhibition of autophagy. *Cancer Res.*, 73, 5985–5995.
26. Singh, K.B. *et al.* (2018) Prostate cancer chemoprevention by sulforaphane in a preclinical mouse model is associated with inhibition of fatty acid metabolism. *Carcinogenesis*, 39, 826–837.
27. Vyas, A.R. *et al.* (2016) Sulforaphane inhibits c-myc-mediated prostate cancer stem-like traits. *J. Cell. Biochem.*, 117, 2482–2495.
28. Dang, C.V. *et al.* (2009) MYC-induced cancer cell energy metabolism and therapeutic opportunities. *Clin. Cancer Res.*, 15, 6479–6483.
29. Hahm, E.R. *et al.* (2016) c-Myc is a novel target of cell cycle arrest by honokiol in prostate cancer cells. *Cell Cycle*, 15, 2309–2320.
30. Xiao, D. *et al.* (2010) Phenethyl isothiocyanate inhibits oxidative phosphorylation to trigger reactive oxygen species-mediated death of human prostate cancer cells. *J. Biol. Chem.*, 285, 26558–26569.
31. Xiao, D. *et al.* (2003) Allyl isothiocyanate, a constituent of cruciferous vegetables, inhibits proliferation of human prostate cancer cells by causing G2/M arrest and inducing apoptosis. *Carcinogenesis*, 24, 891–897.
32. Price, W.S. *et al.* (1996) The manipulation of water relaxation and water suppression in biological systems using the water-PRESS pulse sequence. *J. Magn. Reson. B.*, 112, 190–192.
33. Tkác, I. *et al.* (1999) *In vivo* 1H NMR spectroscopy of rat brain at 1 ms echo time. *Magn. Reson. Med.*, 41, 649–656.
34. Tahata, S. *et al.* (2018) Evaluation of biodistribution of sulforaphane after administration of oral broccoli sprout extract in melanoma patients with multiple atypical nevi. *Cancer Prev. Res. (Phila.)*, 11, 429–438.
35. Wong, N. *et al.* (2014) Changes in PKM2 associate with prostate cancer progression. *Cancer Invest.*, 32, 330–338.
36. Xie, Y. *et al.* (2019) PI3K/Akt signaling transduction pathway, erythropoiesis and glycolysis in hypoxia (Review). *Mol. Med. Rep.*, 19, 783–791.
37. Tao, T. *et al.* (2017) Involvement of EZH2 in aerobic glycolysis of prostate cancer through miR-181b/HK2 axis. *Oncol. Rep.*, 37, 1430–1436.
38. Martin, P.L. *et al.* (2017) Androgen deprivation leads to increased carbohydrate metabolism and hexokinase 2-mediated survival in Pten/Tp53-deficient prostate cancer. *Oncogene*, 36, 525–533.
39. Wang, L. *et al.* (2014) Hexokinase 2-mediated Warburg effect is required for PTEN- and p53-deficiency-driven prostate cancer growth. *Cell Rep.*, 8, 1461–1474.
40. Giannoni, E. *et al.* (2015) Targeting stromal-induced pyruvate kinase M2 nuclear translocation impairs oxphos and prostate cancer metastatic spread. *Oncotarget*, 6, 24061–24074.
41. Singh, S.V. *et al.* (2012) Cancer chemoprevention with dietary isothiocyanates mature for clinical translational research. *Carcinogenesis*, 33, 1833–1842.
42. Kim, S.H. *et al.* (2009) D,L-Sulforaphane causes transcriptional repression of androgen receptor in human prostate cancer cells. *Mol. Cancer Ther.*, 8, 1946–1954.
43. Gao, L. *et al.* (2013) Androgen receptor promotes ligand-independent prostate cancer progression through c-Myc upregulation. *PLoS One*, 8, e63563.
44. Labbé, D.P. *et al.* (2018) Transcriptional regulation in prostate cancer. *Cold Spring Harb Perspect Med.*, 8, piia030437.
45. Jamaspishvili, T. *et al.* (2018) Clinical implications of PTEN loss in prostate cancer. *Nat. Rev. Urol.*, 15, 222–234.
46. Singh, K.B. *et al.* (2018) Inhibition of glycolysis in prostate cancer chemoprevention by phenethyl isothiocyanate. *Cancer Prev. Res. (Phila.)*, 11, 337–346.
47. Shankar, S. *et al.* (2008) Sulforaphane enhances the therapeutic potential of TRAIL in prostate cancer orthotopic model through regulation of apoptosis, metastasis, and angiogenesis. *Clin. Cancer Res.*, 14, 6855–6866.
48. Shafi, A.A. *et al.* (2015) Differential regulation of metabolic pathways by androgen receptor (AR) and its constitutively active splice variant, AR-V7, in prostate cancer cells. *Oncotarget*, 6, 31997–32012.
49. Khurana, N. *et al.* (2017) Multimodal actions of the phytochemical sulforaphane suppress both AR and AR-V7 in 22Rv1 cells: advocating a potent pharmaceutical combination against castration-resistant prostate cancer. *Oncol. Rep.*, 38, 2774–2786.
50. Liang, J. *et al.* (2019) Sulforaphane as anticancer agent: a double-edged sword? Tricky balance between effects on tumor cells and immune cells. *Adv. Biol. Regul.*, 71, 79–87.